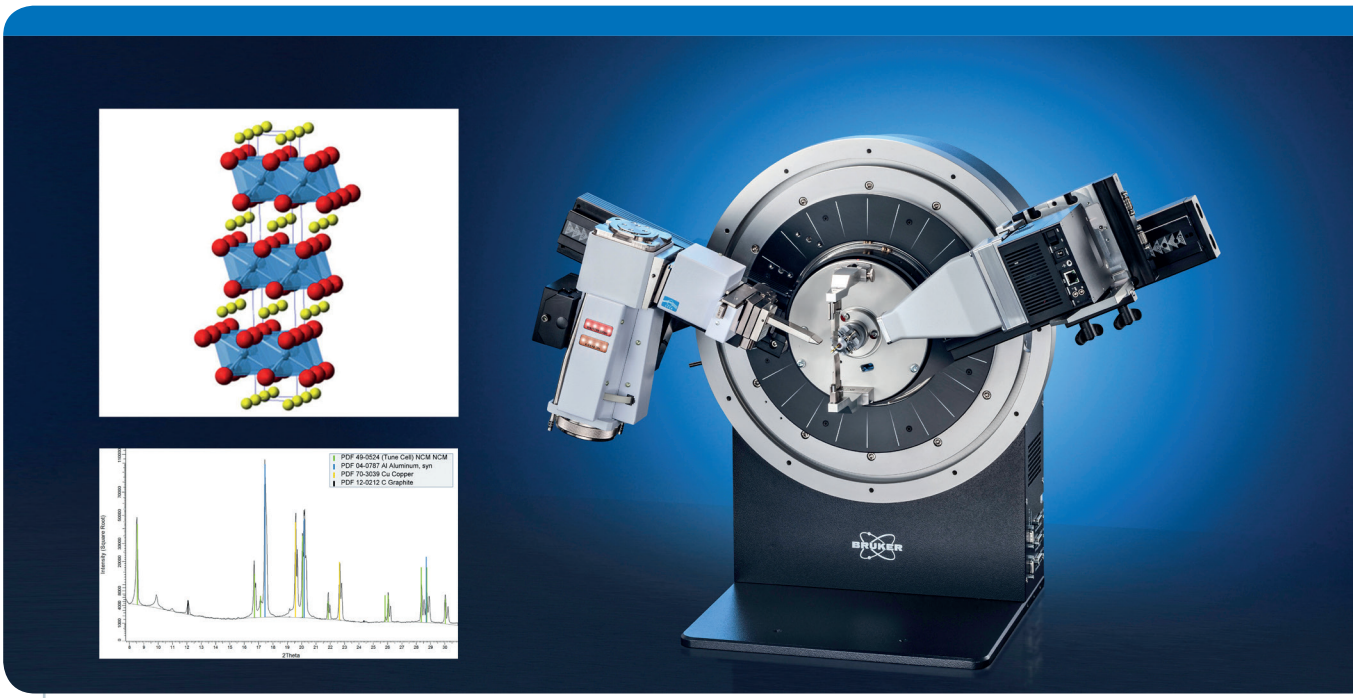

Lab Report XRD 91

In Operando XRD of Battery Pouch Cells

- Characterization of an NMC pouch cell with the EIGER2 R 500K

Pouch cells have become an industry standard battery design due to their efficient shape and lightweight construction. In operando measurements allow simultaneous monitoring of the cathode and anode for cycling effects which effect energy storage performance. This lab report describes in operando characterization of an NMC pouch cell using XRD with the D8 ADVANCE equipped with Mo radiation and the EIGER2 R 500K detector.

The pouch cell used in this experiment was made of a single NMC ($LiNi_xMn_yCo_zO_2$) layer (67 µm) coated on Al foil (15 µm), a separator (40 µm), and graphite (82 µm) coated on Cu foil (9 µm). The electrodes were immersed in a $LiPF_6$ electrolyte solution, and packed in a polymer-Al composite bag. The pouch cell was positioned in the center of the diffractometer, held by two clamps. The total thickness of the pouch cell was about 920 µm. Mo radiation rather than the more common Cu radiation was used for the transmission measurements to reduce the effects of X-ray absorption by the pouch cell. The thick Si sensor of the EIGER2 R 500K is well suited for wavelengths ranging from Cr to Mo, producing high signal while reducing the background by minimizing the effects of charge sharing.

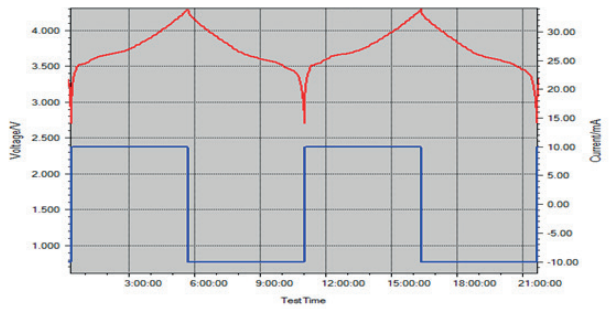

Figure 1: Charge/discharge profile showing the evolution of the cell voltage (red) with applied current (blue).

Two charge/discharge cycles were done at C/5 rate (5 hr charge, 5 hr discharge), leading to a total cycling time of 20 hours. The pouch cell was charged at constant current, the charge/discharge profile is shown in figure 1.

Diffraction data were collected during charge/discharge cycling. For this particular experiment, diffraction patterns were collected in transmission geometry from 7-32° 2θ. This angular range was covered in a single shot with the EIGER2 R 500K detector. This allows for fast data collection with only 3 min per diffraction pattern, resulting in 400 diffraction patterns collected over the 20 hr experiment. The fine time slicing provides detailed insight on the structural changes happening during the cycling process. The excellent data quality and high intensity of the individual diffraction patterns suggest that data collection time could be reduced below 1 minute.

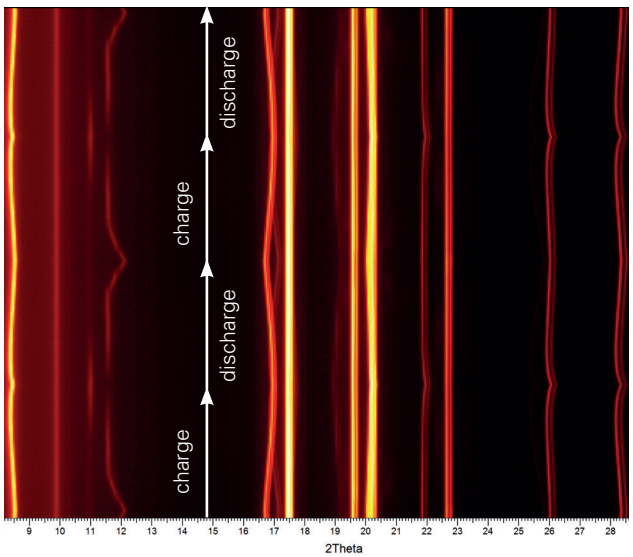

Figure 2: Iso-intensity plot of the two charge/discharge cycles with DIFFRAC.EVA.

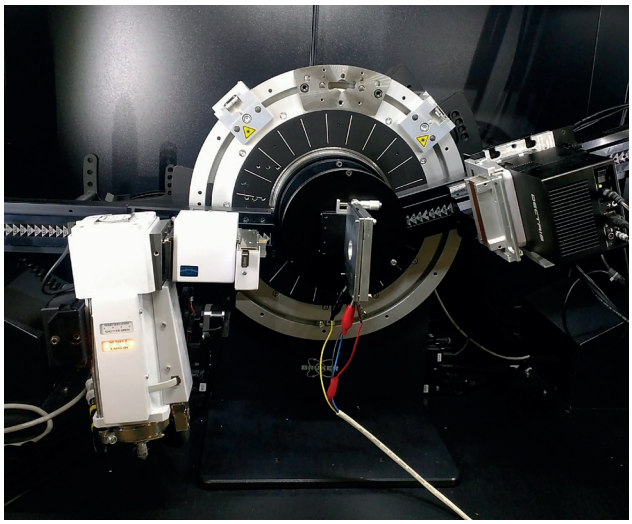

Figure 3: Set-up of the D8 ADVANCE used for the in-operando charge/discharge experiments.

Table 1. D8 ADVANCE configuration
Mo radiation (0.71 Å, 17.5 keV)
Focusing Goebel mirror, 1 mm slit, 2.5° primary axial Soller
Pouch cell – 2 charge/discharge cycles at C/5 rate
2.5° panoramic axial Soller EIGER2 R 500K detector, 2θ-optimized mode, 180 mm sample-to-detector distance

During charging Li^+ ions migrate from the positive electrode to the negative electrode, where they intercalate in the graphite layers. This process is reversed upon discharge. The iso-intensity plot in figure 2 displays that the phase composition changes reversibly upon cycling. Figure 4a shows a qualitative phase analysis on a diffraction pattern taken at 2.7 V (discharged state), figure 4b at 4.3 V (charged state). As expected, LiC_6 and other Li/C phases resulting from the Li intercalation are present in the charged state (figure 4a) but absent in the discharged state (figure 4b).

Beyond this qualitative information, more detailed information can be extracted from a Rietveld refinement. A typical in operando experiment will consist of several hundreds or even thousands charge/discharge cycles, hence automated batch mode evaluation is essential to efficiently analyze the large number of diffraction patterns. In this case, all 400 patterns were analyzed in DIFFRAC.TOPAS using batch mode. For a proper Rietveld refinement, the sandwiched layer pouch cell design has to be taken into account including peak intensity corrections, profile and position corrections[1].

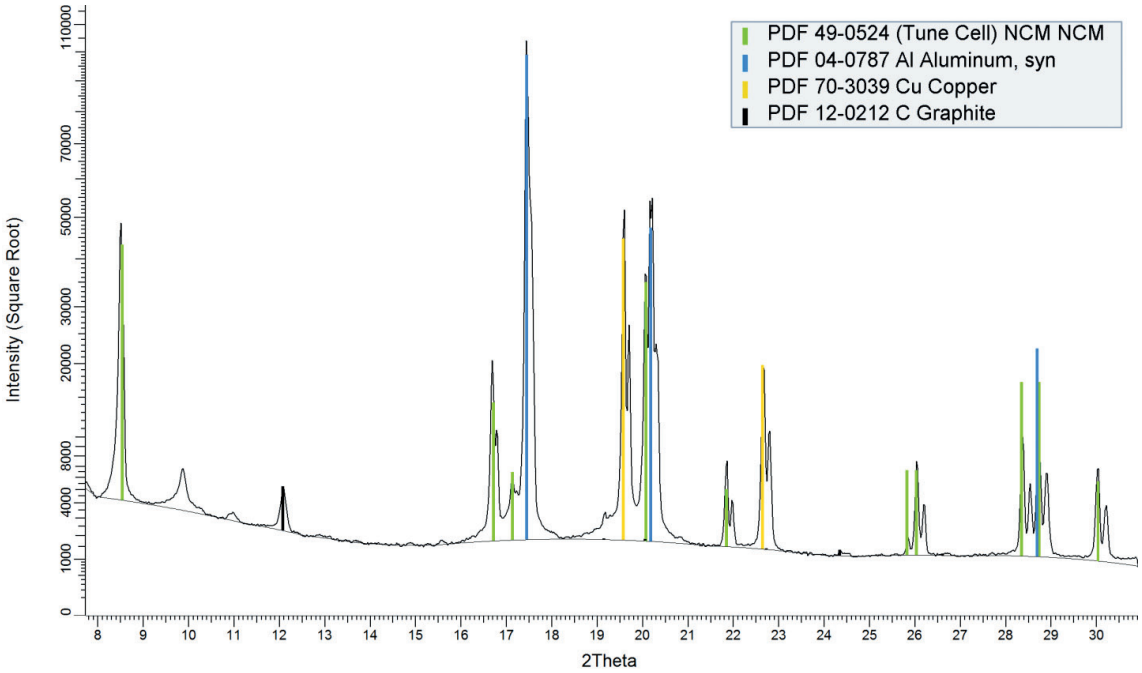

Figure 4a: Qualitative phase analysis with DIFFRAC.EVA of a diffraction pattern collected at 2.7 V (discharged state). The y axis is displayed in square-root scale to emphasize the weak diffraction peaks of minor phases. The peak at 9.5° 2θ is from the separator between anode and cathode.

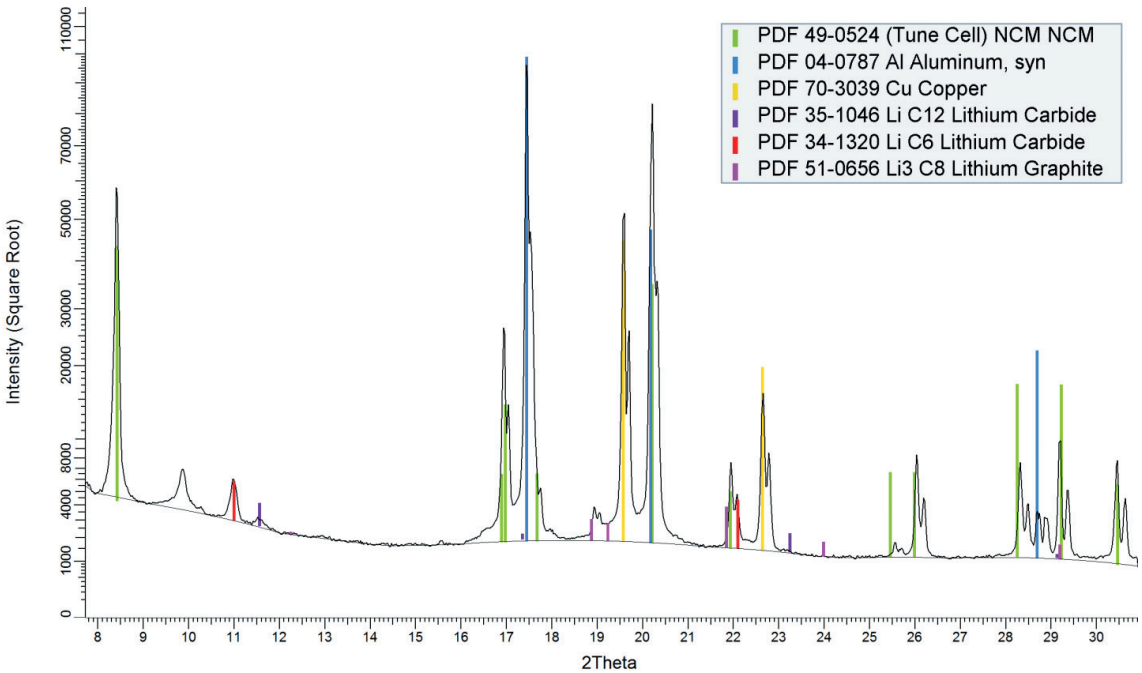

Figure 4b: Qualitative phase analysis with DIFFRAC.EVA of a diffraction pattern collected at 4.3 V (charged state). The y axis is displayed in square-root scale to emphasize the weak diffraction peaks of minor phases. The peak at 9.5° 2θ is from the separator between anode and cathode.

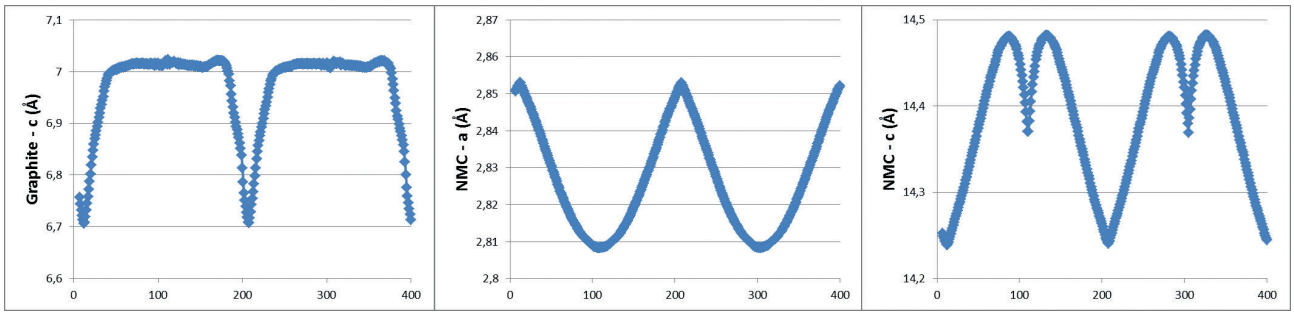

Figure 5: Evolution of the graphite and NMC lattice parameters as a function of the state of charge for the two charge/discharge cycles.

Figure 5 shows the NMC and graphite lattice parameters during the two charge/discharge cycles.

The intercalation of Li into the layered graphite structure during charge initially leads to a quick expansion of graphite *c*-lattice parameter and LiC_X (X = 24,12,6) were formed and identified as charging continues.

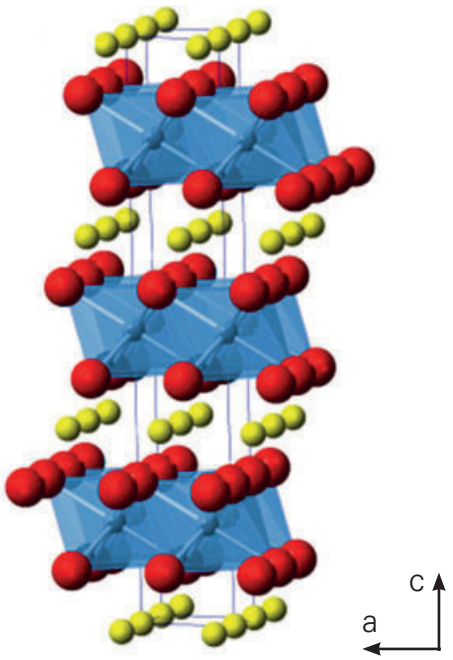

Figure 6: Layered structure of NMC; Li (yellow), O^{2-} (red), *M* (blue).

Interestingly, the NMC *a*- and *c*-lattice parameters show opposite behavior during cycling. The *a*-lattice parameter decreases during charge, as intuitively expected since Li transfers from NMC to graphite. The *c*-lattice parameter shows a strong initial increase during charge, followed by a decrease just before reaching its maximum capacity. This behavior is linked to the layered structure of NMC. Figure 6 shows that the metal atoms (Ni, Mn and Co) are arranged in layers of MO_6 octahedra stacked along the *c*-axis with Li atoms in-between. During charge, Li leaves the structure leading to strong O–O electrostatic repulsion. As a consequence, the *c*-lattice parameter expands. The then following reduction of the *c*-axis at higher charge levels (at > 4V) can possibly be linked to a charge transfer from oxygen to the transition metals, which would reduce again the O-O electrostatic repulsion. At the same time, the transition metal oxidation state increases, reducing the radii of the metal ions and resulting in a stronger *M*-O attraction. This primarily affects the MO_6 layers in the *ab*-plane and explains the decrease of the *a*-lattice parameter.

This lab report demonstrates that a wealth of structural information can be obtained from in operando studies on battery materials using a D8 ADVANCE diffractometer equipped with Mo radiation and the EIGER2 R 500K detector. Efficient data collection strategies allow for fine time slicing, providing detailed insight on the structural changes happening during the cycling process.

References

[1] Rowles, M.R. & Buckley, C.E. (2017), J. Appl. Crys. 50, 240-251

Bruker AXS GmbH

info.baxs@bruker.com

Worldwide offices

bruker.com/baxs-offices

Online information

bruker.com/xrd

www.bruker.com